Test Simulation of Neutron Damage to Electronic Components using Accelerator Facilities

D. King[1], E. Bielejec[1], C. Hembree[1], K. McDonald[1], R. Fleming[1], W. Wampler[1], G. Vizkelethy[1], T. Sheridan[1], V. Harper-Slaboszewicz[1], P. Griffin[1]

[1] Sandia National Laboratories, USA

Email contact of main author: dbking@sandia.gov

Abstract. The concept of "equivalent" damage in electronics when comparing accelerator and fast neutron irradiation is a topic of much interest. Sandia National Laboratories has an ongoing effort to use accelerator facilities to simulate transient defect populations generated from displacement damage and ionization effects observed in electronics at fast burst neutron facilities. This paper examines the utility of two accelerator facilities that will be used to simulate neutron induced damage and ionization when performing transistor tests. Physics based modeling comparisons of the test results will also be presented.

1. Introduction

Historically, fast burst neutron facilities have been used to study the early-time transient response of electronics to displacement damage and ionization. With the closure of most fast burst neutron facilities in the United States, a new test methodology is being developed that consists of high-fidelity computational models combined with testing of electronics at alternative experimental facilities such as the Sandia National Laboratories (SNL) Ion Beam Laboratory (IBL), the SNL Annular Core Research Reactor (ACRR), and the Little Mountain Test Facility (LMTF) linear accelerator. The computational models are initially validated at the fast burst neutron facilities and then applied to the test results at alternative facilities. Ultimately, when fast burst neutron facilities are not available, tests at alternate facilities, combined with computational models, will be used to simulate fast burst neutrons. This new methodology of combining computational models and tests at the alternate facilities will allow a complete representation of the physics parameters needed to correlate the early-time transient behaviour of defects generated by displacement damage in conjunction with ionization effects. The use of multiple facilities requires that the modelers and experimentalists understand how damage in one facility relates to damage in the other alternate facilities. The selection of appropriate damage metrics is the key to understanding these damage relationships. The successful implementation of the modeling/testing methodology would allow the prediction of electronic response under a wide variety of radiation conditions.

Our program has successfully completed a series of experimental tests that compare single transistor damage metrics and response at the fast burst neutron and alternate facilities [1-4]. This paper presents a test and modeling methodology that will aid in determining how best to use alternate facilities along with circuit simulation codes to assist us in predicting transistor response in fast burst neutron facilities. We are primarily interested in displacement damage and ionization (both dose and dose rate) as they affect individual transistors. We will demonstrate that alternate facilities, such as the IBL and LMTF, have great utility in replacing

[1] Sandia National Laboratories is a multiprogram laboratory operated by Sandia Corporation, a Lockheed-Martin Company, for the United States Department of Energy's National Nuclear Security Administration under contract DE-AC04-94AL85000.

the use of fast burst neutron facilities when testing radiation damage to bipolar semiconductors and the appropriate damage metrics are selected.

2. Fast Burst Neutron and Alternate Facilities

The neutron irradiations were performed at the SPR-III central cavity over a wide range of neutron fluences. SPR-III is a fast burst reactor, which can be operated in either a steady-state or pulsed mode. A maximum total neutron fluence of $5x10^{14}$ n/cm^2 [$3.9x10^{14}$ n/cm^2 1 MeV (Si) equivalent], maximum dose of 120 krad(Si), and a full-width-at-half-maximum (FWHM) of 100 μs is possible in single pulsed mode. The devices were placed in the SPR-III central cavity to achieve maximum neutron fluence and because the neutron spectrum is a relatively unmoderated, well characterized, fast ^{235}U fission spectrum. The operation of the transistors was monitored prior to, during, and for 100 seconds after each shot.

The LMTF is a linear accelerator (LINAC) operated in electron beam mode. This facility is used in our test methodology process to bound the contribution of ionization rate effects to the device and circuit performance. LMTF has a unique capability among LINACs in that it can provide long, up to 50 microsecond, pulse widths. Pulse widths can be tailored from 50 nsec to 50 μsec with beam currents ranging from 0.05 to 2 Amps. The electron beam peak energy can be tuned from 5 to 30 MeV. Ionizing dose rates from 5E6 to 4E13 rad(Si)/sec are achieved through the use of a variety of diffusers, target positions, and pulse widths. Useful electron beam diameters (with ~ 80% uniformity) range from ~1.5 cm for high dose rates to 30 cm for low dose rates. The LMTF can operate with a maximum repetition rate of 2 pulses per second.

The IBL is a DOE user facility for ion beam analysis (IBA) and radiation effects microscopy (REM). With three accelerators, a 6 MV tandem Van de Graaff (including an RFQ booster for gold ions at 380 MeV), a 3 MV single ended Van de Graaff, and a 350 KV Cockroft Walton, numerous ion sources and multiple dedicated beam-lines, the IBL can provide a wide variety of IBA and REM techniques. For this particular application, a high flux of ion irradiations to simulate a fast burst reactor environment, we have modified our beam-line to achieve a 1 x 1 mm^2 spot size with excellent uniformity over the central region of the spot (covering the active region of a bipolar transistor) with the increased beam currents necessary to provide sufficient flux on target to match or exceed the defect creation rates observed in fast burst neutron facilities (namely SPR-III with a 5E18 n/cm^2/s peak flux of 1-MeV Silicon equivalent neutrons). For the experiments discussed in this paper we used a Silicon ion beam with a range of energies designed to: (1) maximize defect formation at the base-emitter junction of the device (EOR) or (2) to achieve uniform displacement damage over the active region of the device (the base-emitter junction through the neutral base).

Displacement damage results when an incident particle (either a neutron or ion) creates silicon recoils that move from their original lattice sites. This silicon recoil atom then undergoes further collisions with other lattice atoms creating a collision cascade. This results in the formation of Frenkel pairs (vacancy interstitial pairs) in the silicon bipolar junction transistors, which shorten carrier lifetime and degrade the transistor gain. One of the key differences between ion and neutron irradiations is the method by which they transfer energy to the silicon lattice. Neutrons have a very small collision cross-section with Si atoms (no Coulomb interaction); therefore, most neutrons pass through the device without striking a Si atom. Those neutrons that do strike a Si atom produce a scattered or transmuted

lattice ion with a significant recoil energy and then cause localized collision cascades; therefore neutron damage is created uniformly throughout the device. Ions strike the front surface of the transistor and proceed to lose energy continuously as they travel through the device by Coulomb scattering (interaction with the target nuclei) and ionization (interaction with electrons). The net result is that, for incident ions, Frenkel pair creation varies as a function of penetration depth with a majority of the displacement damage created at the end-of-range of the ion trajectory. Photocurrent generation also varies as a function of penetration depth with a majority of the photocurrent created in the initial ion track before the end-of-range of the ion trajectory.

3. Simulation Codes

For the work reported in this paper, we used the two computational codes described below: an atomistic model code for discrete component irradiations (1D) and a circuit simulator (Xyce). An atomistic model code, 1D, is used to model the static and dynamic changes in gain of a silicon bipolar transistor due to energetic particle irradiation. This includes the time-dependent annealing of the primary defects (silicon interstitials and vacancies) produced directly by the irradiation and the resulting recoil products as well as the transformation of these primary defects into more stable defect configurations, such as a divacancy and a vacancy-phosphorous complex. These defects influence transistor operation through capture and emission of electrons and holes. The model follows the local concentrations of electrons, holes and lattice defects of various types and charge states. Local concentrations of these are evaluated by numerical solution of coupled differential equations describing diffusion and drift of the mobile species, with carrier emission and capture, and defect reactions. This type of explicit treatment of the transient effects of defect reactions on gain is not provided by commercially available device simulation packages. This model provides a physics-based approach to simulate these effects and the resulting transient changes in transistor gain.

The Xyce [5] circuit simulator is a high performance SNL developed SPICE compatible tool which allows the simulation of very large circuits through parallelization. Although Xyce is a circuit simulator, it can also be used to model simple circuits with a single transistor and bias resistors. Xyce is often used in lieu of 2D codes because its execution time is minutes instead of hours for a single simulation; this short execution time allows many modeling simulations to be performed for parametric studies. Xyce incorporates radiation models for both photocurrent and displacement damage effects. Photocurrent effects can result when ionizing radiation generates electron-hole pairs within a semiconductor device and is produced when excess carriers are accelerated by an electric field, typically occurring when carriers are created inside pn junctions, or when they diffuse into them. Incident radiation particles damage the semiconductor lattice by creating crystalline defects. These defects reduce carrier lifetimes, by adding recombination centers in the energy bandgap of the material. The dominant effect is transistor gain reduction. The neutron model implemented in Xyce is based on adding a reaction model to the standard Gummel-Poon BJT equations and consists of a set of defect species and time-dependent reactions between those species. Carrier emission and capture reactions are included in the model.

4. Experimental Details

Single diffusion lot 2n2222 npn bipolar junction transistors from Microsemi were used in these experiments to minimize and control the device to device variation present in

commercial off-the-shelf (COTS) parts. Construction analysis, secondary ion mass spectroscopy (SIMS), and spreading resistance profile (SRP) measurements were performed on these devices to accurately determine the device geometry and doping profile of the active region of the devices. These parameters are extremely important for understanding and modeling the defect formation and transport during both ion and neutron irradiations. 2n2222 devices were chosen for these experiments because they are a well-established technology, and silicon has a considerable history of documented defect literature and extensive data base.

The setup for single transistor testing is shown in Figure 1 with red letters that indicate the measurement points. The transistor, Q, was operated in constant emitter current mode, provided by a current limiting diode, CLD, biased to -15 V (VEE) on the emitter leg. The base-collector junction is reverse-biased with 10 V (VCC) on the collector. The base leg is tied to ground through a relatively large resistor (RB) to ensure an accurate measurement of the base current prior to the shot. The additional clipping diode, D, located on the base leg was used to prevent large base potential excursions due to the large photocurrent response during the ion and electron beam irradiations. The currents of the transistor were monitored using current viewing resistors (RB, RC, RE) before, during, and after the shots. The voltages across the current viewing resistors were recorded with a Yokogawa DL750P oscilloscope. This circuit was used at IBL and LMTF to measure displacement damage and ionization effects. For SPR-III operations, the circuit described above was modified by removing the clipping diode from the base leg.

Figure 2 illustrates the collector and base current behavior (IC and IB, respectively) of a 2n2222 bipolar junction transistor with a nominal constant emitter current bias of 0.2 mA for the SPR-III irradiation. The combined gamma/neutron ionization during the pulse causes an increase in IC (from 0.2 mA to 4.6 mA) and IB (from 2 μA to -3 mA) due to the photocurrent generated in the transistor junctions by the ionization. The neutron degradation is masked during the pulse by the transient photocurrent. The circuit measuring convention defines the photocurrent response in IC to be positive and in IB to be negative. As the ionization component of the pulse decreases, the neutron damage effect on IC and IB becomes evident. IC decreases from a nominal current of 0.2 mA to 0.05 mA. IB increases from 2 μA to 0.18 mA. As the neutron component of the pulse decreases, both IB and IC begin to anneal. IB decreases and IC increases after the pulse during the anneal phase.

The collector and base current responses for a 10-MeV Si irradiation are pictured in Figure 3. The 10-MeV Si irradiation generates peak photocurrents that are similar in magnitude to those observed at SPR-III. Although the IBL generates a square wave pulse, we see that the photocurrent magnitude decreases during the pulse. Displacement damage reduces carrier lifetime and photocurrent magnitudes. At the pulse end, the ion damage effect on IC and IB becomes evident. IC decreases from a nominal current of 0.2 mA to 0.03 mA. IB increases from approximately 2 μA to 0.2 mA.

In prior work [1-4], we have demonstrated that the annealing factor (defined as the change in the reciprocal transistor gain at any time during a test compared to the change in the reciprocal transistor gain at late time) is almost identical for silicon ion irradiations over a wide range of incident energies and fast neutron irradiations at the Sandia pulsed reactor (SPR-III) for equivalent neutron/ion fluence. Figure 4 illustrates the annealing factors for a SPR-III test and a 10 MeV silicon ion IBL test. The comparison indicates good agreement between the time dependence of the change in the device gain and the defect population

generated by the ion and neutron irradiations. These tests, in conjunction with late-time Messenger-Spratt studies, have allowed us to develop "ion fluence to effective 1-MeV(Si) equivalent neutron fluence" conversion factors. For most of our discrete component irradiations, the photocurrent generation was a secondary effect, the post-irradiation gain values were dominated by displacement damage effects. However, we did observe photocurrent effects from the tail of a SPR-III pulse that masked displacement damage response at test times less than 1 ms for low emitter current configurations. We believe that photocurrent effects will be more important where we have interplay between various discrete components as would be found in a complex circuit employing a number of discrete components. As a result, we have started testing and modeling efforts to better understand photocurrent effects in discrete transistors at both LMTF and the IBL.

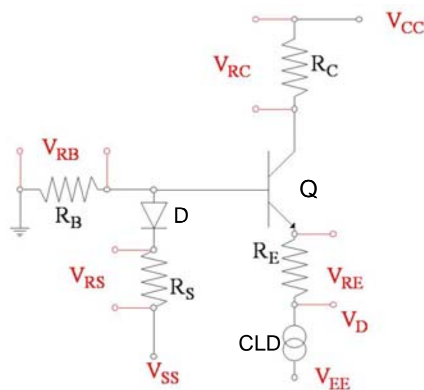

FIG. 1. Single transistor test circuit.

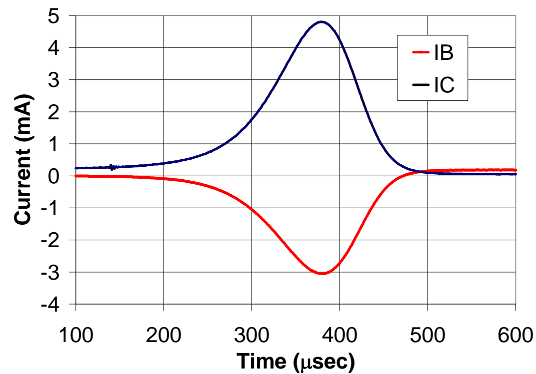

FIG. 2. Base and collector current response to a maximum pulse at the SPR-III facility. The nominal emitter current is 0.22 mA.

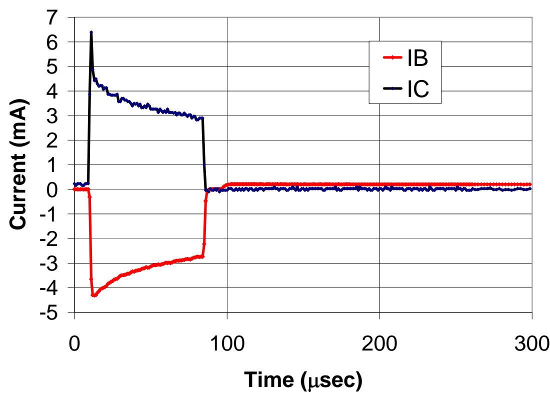

FIG. 3. Base and collector current response to a 10 MeV Si ion pulse at IBL. The nominal emitter current is 0.22 mA.

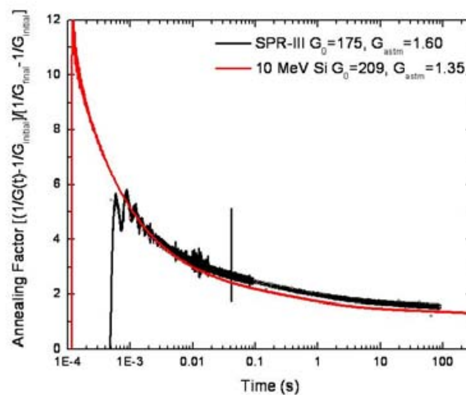

FIG. 4. Annealing Factor comparison with IBL and SPR.

4.1. IBL Single Transistor Photocurrent Tests

The IBL allows us to vary the ratio of photocurrent generation to displacement damage via the choice of ion and energy combination. For the npn transistors irradiated in this work, 4.5 and 10 MeV Si ion irradiation will maximize the effective displacement damage near the emitter-base junction while minimizing the photocurrent generation, whereas, a 36 MeV Si irradiation will maximize the photocurrent generation. All irradiations will have significant displacement damage effects in contrast to LMTF irradiations where we only have

photocurrent generation. Figure 5 illustrates the photocurrent generated in the 2N2222 bipolar transistor at the IBL for 4.5, 10, and 36 MeV Si ion irradiations. As described above, the photocurrent peak increases by roughly an order of magnitude with increasing ion energy. End-of-range for a 4.5 MeV Si ion occurs near the base-emitter junction; photocurrent production occurs in the base emitter junction. End-of-range for the 10 MeV Si ion occurs near the base collector junction; photocurrent production occurs in and near the base collector junction. End-of-range for a 36 MeV Si ion occurs deep in the substrate; photocurrent is generated in and near the base collector junction as well as the collector and substrate.

For the rest of this paper we will concentrate on the 36 MeV Si irradiations as this case most closely mimics the electron beam irradiations using a high energy electron LINAC. We plot in Figure 6 the peak IBL photocurrent as a function of ion flux. One of the open questions with the ion irradiations is the magnitude of the ion induced ionization effects – how many electron-hole pairs are being created and how many recombine? We address this issue by calibrating our ion beam induced photocurrent generation with photocurrents from the LMTF.

4.2. **LMTF Single Transistor Photocurrent Tests**

We use the LMTF facility to decouple displacement damage and ionization effects that are simultaneously observed in bipolar transistors at a fast burst neutron facility. While the gain degradation due to ionization is an order of magnitude less than that of displacement damage for the test conditions described in this paper, their effect must be understood. Photocurrents generated in the base-collector junction of a bipolar transistor have a significant effect on the measured currents and it is extremely important that they be addressed in the modeling.

At the LMTF we have tested transistors at dose rates ranging from 5E7 to 1.5E10 rad(Si)/sec using pulse widths that vary from 1 to 50 μsec. Total dose varied from 100 to 50000 rads(Si). Dose rates experienced by electronics at fast burst reactors typically range between 1E8 and 1E9 rads(Si)/sec. Dose can range from 10 to 100 krad(Si). Figure 7 shows the photocurrent generated at LMTF as a function of dose rate for 50 μsec pulse widths. The range of dose rate was selected to match photocurrents generated at the IBL with 36 MeV Si ions. Photocurrents at IBL and LMTF from Figures 6 and 7 can be matched to calculate an IBL-to-LMTF photocurrent conversion factor as shown in Figure 8. The photocurrent conversion factor, in this case, is 1.27E-4 rad(Si) cm^2/ion. This factor is of critical importance as it allows for an understanding of the effective dose rates that we have during IBL irradiations. The IBL-to-LMTF photocurrent conversion factor depends on the device geometry, the ion species used, and the energy of the irradiation.

5. IBL and LMTF Photocurrent Modeling Results

Xyce has traditionally been used to characterize photocurrents at LINAC facilities such as LMTF. Figure 9 shows a Xyce simulation of a LMTF shot with a pulse width of 5 μsec and a dose rate of 1E9 rad(Si)/sec. These 5 μsec pulses have contributions from prompt and delayed photocurrents and are thus considered ‘long’ pulses. The transistor modeled is a Microsemi 2N2222.

Figure 10 illustrates the photocurrent generated in the a bipolar transistor (IB) at LMTF with a dose rate of 1E10 rad(Si)/s and at the IBL with a 36 MeV silicon ion flux of 1.07E14 ion/cm^2/s. Furthermore, we plot the photocurrent generation as predicted by both 1D and Xyce for the same experimental parameters. The 1D code has the ability to simultaneously

model both photocurrent generation and displacement damage as well as simulating the transient annealing of the displacement damage. These code results accurately reproduce the experimental IBL data. The Xyce simulation is bounded by the IBL and LMTF tests; at this time, Xyce has not implemented the synergy between the displacement damage and photocurrent interactions as are implemented in the 1D code. Overall, we find excellent agreement between the discrete component irradiations and the simulation codes within the constraints of their as-implemented capabilities.

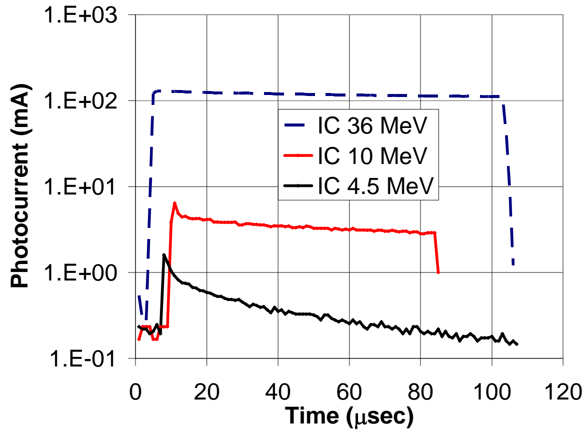

FIG. 5. Photocurrent magnitude as a function of ion energy at IBL.

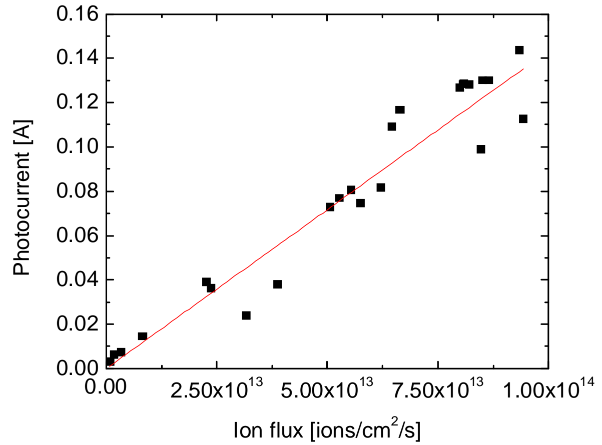

FIG. 6. Ion flux rate dependence of photocurrent generated at the IBL.

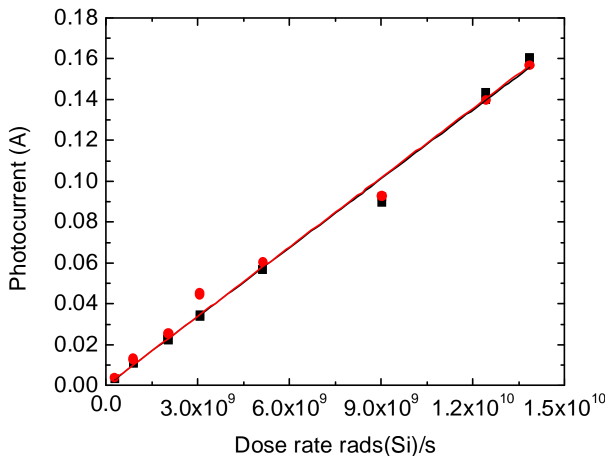

FIG. 7. Dose rate dependence of photocurrent generated at the LMTF.

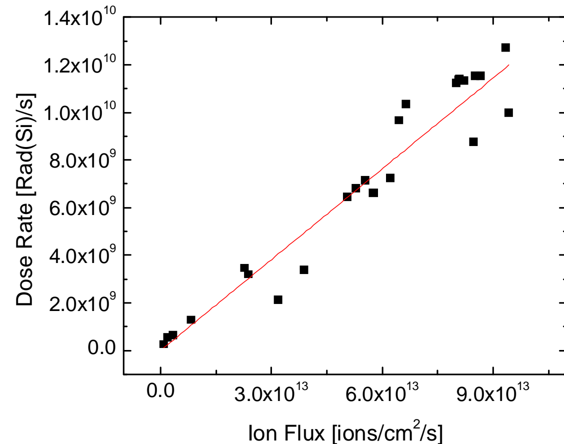

FIG. 8 Photocurrent conversion factor for IBL and LMTF.

6. Conclusions

SNL has an ongoing effort to use accelerator facilities to simulate displacement damage and ionization effects observed in electronics at fast burst neutron facilities. The effort also depends on the use of high fidelity computational models to confirm our ability to predict displacement damage and ionization effects at accelerator and neutron facilities. We have presented preliminary LMTF and IBL test and computational results of displacement damage and photocurrent for single transistors. We observed excellent agreement between the experimental results and preliminary Xyce and 1D photocurrent calculations at LMTF and

IBL. Ultimately, we seek to establish a correlation between the device damage, including displacement as well ionization effects, observed in neutron and in ion beam radiation environments and to validate the ability of our computational tools to predict device and circuit response under either type of radiation.

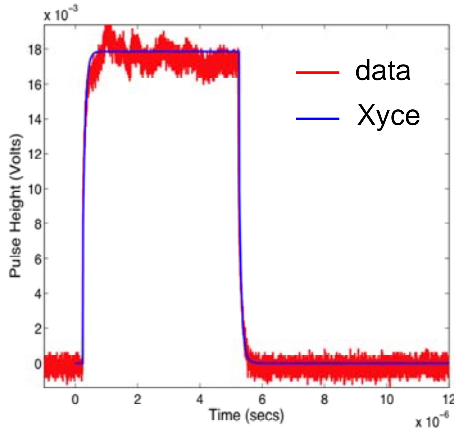

FIG. 9. Xyce photocurrent simulation at LMTF.

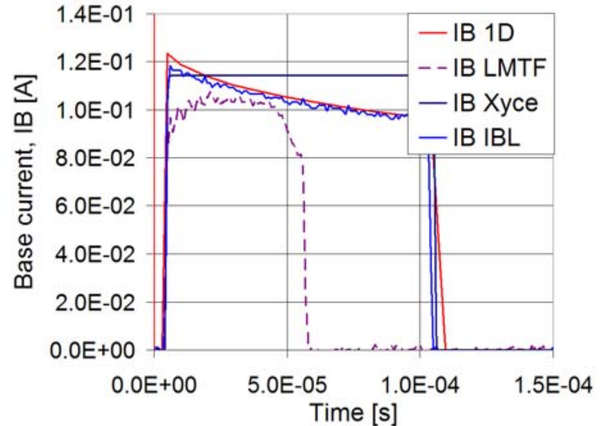

FIG. 10. Simulated and test photocurrent comparisons at LMTF and IBL.

ACKNOWLEDGMENTS

We acknowledge the outstanding support of D. L. Buller in running and maintaining the IBL and the members of the SNL experimental team.

8. References

[1] E. Bielejec et al., "Damage Equivalence of Heavy Ions in Silicon Bipolar Junction Transistors", *IEEE Trans. Nucl. Sci.,* vol. 53, pp 3681-3686, Dec. 2006.
[2] E. Bielejec, G. Vizkelethy, R. M. Fleming and D. B. King, "Metrics for Comparison between Displacement Damage Due to Ion Beam and Neutron Irradiation in Silicon BJTs", *IEEE Trans. Nucl. Sci.,* vol. 54, pp 2282-2287, Dec. 2007.
[3] D. B. King, E. Bielejec, P. J. Griffin, K. J. McDonald, P. J. Cooper, R. M. Fleming, "Variability in Damage Equivalence Metrics between Heavy Ions and Neutrons", Proc. 8th International Topical Meeting on Nuclear Applications of Accelerators, Pocatello, Idaho, USA, pp 283-291, American Nuclear Society, ISBN 0-89448-054-5, (2007).
[4] E. Bielejec, G. Vizkelethy, R. M. Fleming W. R. Wampler, S. M. Myers and D. B. King, "Comparison between Experimental and Simulation Results for Ion Beam and Neutron Irradiations in Silicon Bipolar Junction Transistors", *IEEE Trans. Nucl. Sci.,* vol. 55, pp 3055-3059, Dec. 2008.
[5] E. R. Keiter, et al, "Xyce Parallel Electronic Simulator: Reference Guide, Version 4.1", SAND2008-6459, Sandia National Laboratories, Albuquerque, NM, 2008.